494: Temporal and spatial partitioning of measured urban carbon dioxide fluxes

Ben Crawford, Andreas Christen

Department of Geography, University of British Columbia, Vancouver, Canada

Abstract

A 3-year CO_2 flux dataset, flux source area models, and a geospatial dataset are used to develop methods to isolate and model individual CO_2 emissions and uptake processes from a residential neighborhood in Vancouver, Canada. The methods include conditional sampling of 30-minute fluxes to isolate specific processes and take advantage of changing land cover due to varying flux source areas to identify surface and environmental controls on net emissions. Results show that these methods can provide realistic partitioning of the measured net flux into component processes.

Keywords: CO_2 flux, surface heterogeneity, flux source areas

1. Introduction

There is an increasing need to directly monitor greenhouse gas emissions from urban areas to inform and validate inventories and models and to assess emission reduction efforts. Eddy covariance (EC) is a micrometeorological technique that can directly measure net exchange of trace gases at local-scales at fine temporal resolution and there are currently at least 30 urban EC sites in operation throughout the world [1].

The EC method uses instruments located at a single point in the surface layer to make measurements that are representative of the net atmospheric response to forcings from an upwind surface area. This surface area influencing the flux measurement is called the flux source area and it is constantly changing as a function of wind direction, atmospheric stability, and lateral dispersion qualities of the flow [2].

Although it has been demonstrated that urban areas can be considered homogeneous at local scales, dynamic flux source areas in an urban area can potentially contain constantly changing distributions of trace gas source and sink processes depending on micro-scale configurations of emission sources and sinks in the canopy layer. Thus, flux measurements are location-dependent and may not necessarily reflect a true spatial average [3]. In this kind of environment, how this location bias be overcome to determine the 'true' ecosystem behavior? How can measurements from different times and different source areas be compared?

Rather than view location bias as an obstacle, this paper takes the position that surface variability and changing source area composition are advantages that can be leveraged to gain more knowledge about the spatial and temporal patterns and processes contributing to net flux measurements. The objective is to develop methods to isolate and model individual CO_2 processes at fine temporal and spatial resolution using a long-term CO_2 flux dataset in combination with spatial datasets and source area models.

2. Methods

2.1 Sunset eddy-covariance measurements

Net CO_2 fluxes were measured in the Vancouver Sunset neighborhood at a height of 28.8 m on an open, triangular, lattice tower. The surrounding neighborhood is classified as LCZ 9 'open-set lowrise' [4] and has been identified as a representative residential area in a number of previous urban energy and water balance studies.

For this work, three years of continuous EC observations (May 2008 - May 2011) at 30-minute resolution are available. EC instrumentation consisted of an open-path infrared-gas analyzer (Li-7500, Licor Inc., Lincoln, NE, USA) and a sonic anemometer (CSAT 3d, Campbell Scientific, Logan, UT, USA). Three-dimensional wind velocities and CO_2 concentrations were recorded at 20 Hz and fluxes were calculated at 30-minute resolution using block-averaged means, 2-d coordinate rotation, and are corrected for volume and density fluctuations [5]. Additional micrometeorological measurements include incoming solar radiation (26 m, CNR-1, Kipp and Zonen, Delft, Netherlands), canopy air temperature (T_{air}, 2 m, HMP T/RH sensor, Vaisala, Stockholm, Sweden), and soil temperature (T_S, -5 cm, thermocouple).

2.2 Sunset neighborhood spatial dataset

In addition to micrometeorological measurements, a suite of remotely sensed geospatial data was available for this study. A multispectral Quickbird satellite image taken at 2.4 m resolution was merged with airborne LiDAR data at 1 m resolution to extract surface land-cover datasets for a 2x2 km area at 1 m resolution centered on the tower [6]. Land-cover classifications used in this study are: building (λ_B), tree (λ_T), lawn (λ_L), and impervious (λ_I) surface fractions ($m^2\ m^{-2}$).

2.3 Flux source area models

The micrometeorological and geospatial datasets are linked through numerical modeling of flux source areas. The model used for this study requires as input: 30-minute mean wind direction (measured at the tower), surface roughness length (determined from surface morphometry from LiDAR data), measured standard deviation of the crosswind velocity, and atmospheric stability (measured Obukhov Length) [7]. The output of the model is an individual source area for each 30-minute flux measurement that is a 2 m x 2 m resolution surface weighted by its probability to contribute to the measured tower flux. The weighted source areas can then be overlaid and multiplied by the landcover dataset to calculate the landcover composition of each individual 30-minute source area.

2.4 Linking process and place

It has been shown that the net CO_2 flux from an urban environment is the sum of biogenic, anthropogenic, and micrometeorological processes operating across a range of temporal and spatial cycles [8]. The local CO_2 budget for Sunset neighborhood can be expressed as:

$$F_C = E_V + E_B + R_H + R_S + (R_V - P) \quad (1)$$

where F_C is the total net CO_2 flux, E_V is emissions from vehicles, E_B is emissions from buildings, R_H is human and animal respiration, R_S is below-ground soil, root, and waste microbial respiration, R_V is above-ground vegetation respiration, and P is CO_2 uptake by vegetation photosynthesis.

With tower-based EC measurements, however, the actual distribution of these surface source and sink processes is not known. The distribution can be inferred through analysis of source area landcover compositions, but the processes in Eq. 1 must first be conceptually linked to a physical area on the surface (Figure 1). Thus observed changes in source area landcover composition may be interpreted as controls on CO_2 emissions processes.

$$F_C = E_V + E_B + R_H + R_S + (R_V - P)$$
$$\lambda_R \quad \lambda_B \quad \lambda_L \quad \lambda_T\lambda_L$$

Figure 1. CO_2 emissions processes are linked to physical space at the surface.

3. Results

3.1 Traffic emissions (E_V)

E_V is expected to be an important emissions source in this neighborhood and fluctuate on daily and weekly cycles following commuter traffic patterns. Based on actual traffic count data, the majority of E_V is also assumed to originate from busy, arterial roads that grid the neighborhood approximately every 800 m while the contribution from small, residential sidestreets is minor.

In order to extract E_V from F_C, 3 road classes were defined based on road width: residential sidestreets (λ_{RR}), Secondary roads (λ_{RS}), and Major roads (λ_{RM}). Next, individual 30-minute periods were selected when $T_{air} > 14^{o}$ C to avoid emissions from space-heating, and for each hour (separately for weekdays (M-F) and weekends (S-S)), a three-dimensional plot was created with λ_{RM} (%) along the x-axis, λ_{RS} (%) along the y-axis, and F_C (μmol m^{-2} s^{-1}) along the z-axis. A linear plane was then fit through the 30-minute datapoints and extrapolated to endpoints of 0% $\lambda_{RS}/\lambda_{RM}$ coverage, and 100% $\lambda_{RM}(\lambda_{RS})$ coverage (Figure 2).

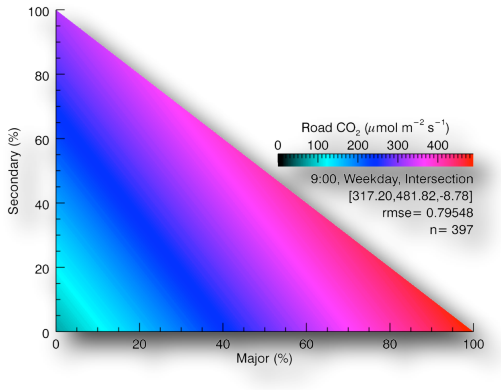

Figure 2. The planar fit E_V model for 9:00 on a weekday.

For each hour, the value at 0% $\lambda_{RS}/\lambda_{RM}$ is deemed to be 'background' emissions ($b = R_H + R_S + R_V + P$). Although b will fluctuate slightly depending on environmental conditions, the simplifying assumption is made that for each hour, b remains constant. This is justified because the various landcover fractions (other than road landcover) remain relatively stable during each measurement, and E_V is at least an order of magnitude greater than the emission terms that contribute to b. Thus, for each hour, E_V can be expressed as:

$$E_V = m_s \cdot \lambda_{Rs} + m_m \cdot \lambda_{Rm} - b \quad (2)$$

where m_s is the planar slope along y-axis and m_m is the planar slope along x-axis *(μmol s^{-1} m^{-2})*.

3.2 Building emissions (E_B)

Approximately 80-90% of buildings in the Sunset neighborhood have natural gas heating systems that generate local CO_2 emissions. The demand for space-heating is expected to be primarily determined by T_{air} as long as T_{air} is below some temperature threshold (T_H). On monthly timescales, there is a linear relation between total emissions and T_{air} [9] and on hourly timescales, E_B is expected to follow a diurnal course depending on occupant activity and T_{air}.

In order to extract E_B from F_C, for each hour, individual 30-minute periods were selected when landcover fractions of major and secondary roads were minimal (< 2 %) in order to avoid the majority of traffic emissions (E_V). This conditional sampling technique was used (rather than statistically modeling and removing E_V) in order to keep the E_V and E_B models independent of each other. Next, to account for different building landcover fractions within each source area, net F_C was divided by λ_B. This step effectively places all measured emissions into the building landcover class and expresses emissions as per unit area of building only.

The 30-minute scaled F_C values were then binned into 2° K T_{air} classes and segmented linear regression was used on bin median F_C values to determine T_H (Figure 3). When $T_{air} < T_H$, E_B increases linearly with decreasing T_{air} (along a slope, m) and when $T_{air} > T_H$, E_B remains constant (m=0) (Figure 4). As with the E_V model, there is some level of background emissions (b) that is assumed constant for each hour. This b is composed of $R_S + R_V + P$ which are assumed negligible when $T_{air} < T_H$, and also R_H and E_V, which are assumed to remain constant for each hour. Thus, for each hour, when $T_{air} < T_H$, E_B can be modeled:

$$E_B = T_{Air} \cdot m \quad (3)$$

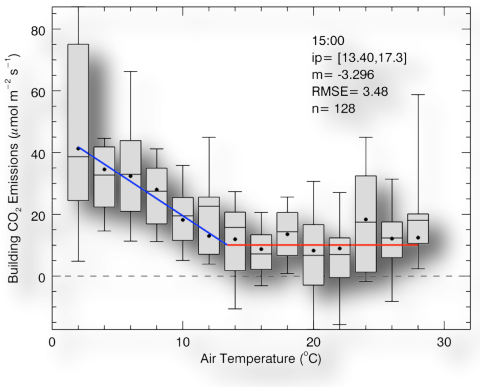

Figure 3. The segmented linear regression E_B model for 15:00. For this hour, T_H = 13.4° C and b = 17.3 μmol m^{-2} s^{-1}. This point is labeled 'ip' in the figure, along with the slope (m) when $T_{air}<T_H$, rmse (μmol m^{-2} s^{-1}), and number of 30-minute datapoints (n).

3.3 Soil respiration (R_S)

To isolate R_S, nocturnal periods when $T_{air}>T_H$ were selected for analysis so that P and E_B are negligible. Additionally, E_V was modeled (Section 3.1) and removed from net F_C, trading model independence for a greatly increased number of datapoints available for analysis. The resulting 30-minute F_C measurements were binned in 1° C T_S intervals and a soil respiration model [10] was fit to the binned F_C medians (Figure 4). Although the T_S range here is limited, previous work in the Sunset neighborhood used soil respiration chamber measurements over representative urban lawns that included measurements across a much broader range of T_S (0° - 30° C) [11]. The model curve generated from the chamber measurements is shown for comparison against the curve fit to the EC measurements (Figure 4).

Although the two methods appear to agree quite well, the chambers were representative of an area composed entirely of lawn, while the EC flux source areas were on average only 32% lawn. To reconcile this difference, the EC soil respiration curve was multiplied by the source area landcover fraction of lawns (λ_L). The residual between the scaled and unscaled curves then must be due to R_H, R_V, and residual emissions from other processes. At 0° C, R_V is assumed to be negligible, so the difference between the scaled and unscaled R_S curves at 0° C is taken to be R_H. The simplification is then made that R_H remains constant.

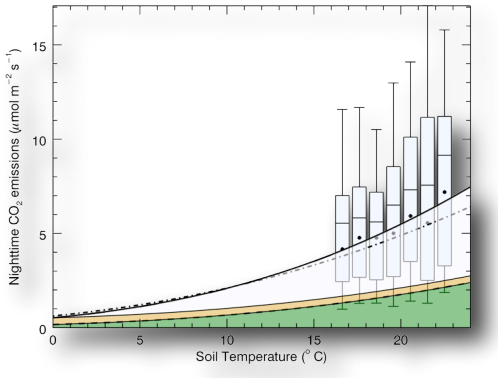

Figure 4. A soil respiration model (solid black curve) is fit to nighttime binned EC F_C medians (black dots). A model fit to chamber measurements is shown as a dashed line for comparison. The green area is the EC R_S model scaled by λ_L, the orange area is R_H, and the gray-shaded area is the residual.

3.4 Photosynthesis (P)

Daytime measurements when $T_{air} > T_H$ were selected to account for the effects of P. Additionally, E_V, R_S, and R_H were modeled and subtracted from F_C measurements and the resulting 30-minute values were sorted by photosynthetic photon flux density (PPFD, 100 μmol m^{-2} s^{-1} bins). A photosynthetic light response curve was then fit to the binned F_C medians [12] (Figure 5).

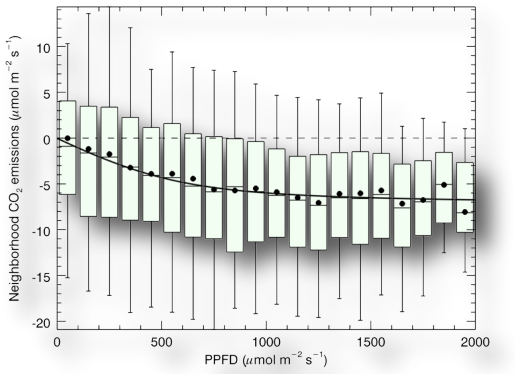

Figure 5. Photosynthetic light response curve (black curve) fit to binned F_C medians (black dots).

4. Conclusions

Methods to isolate and model individual CO_2 emissions processes using net CO_2 EC flux measurements, source area models, and surface datasets have been developed. Each component was then modeled at hourly resolution over a complete year from May 2011-May 2012 (Figure 6). This period was withheld from model development to be used as a validation dataset.

To compare observations and models, the 30-minute model results for each emissions process were scaled by its corresponding land-cover composition (Figure 1) determined from source area modeling. It remains to be seen how accurate the individual models are, though comparisons against observed daily totals are encouraging (Figure 7).

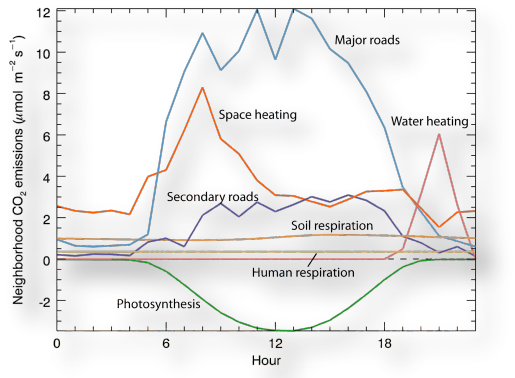

Figure 6. Ensemble hourly averages for modeled F_C processes for an entire year. The water heating model was not described in the text, but is derived from the residual emissions from the E_B model when T_{air}=T_H.

5. Acknowledgements

This research was part of the Environmental Prediction in Canadian Cities (EPiCC) Network, funded by the Canadian Foundation for Climate and Atmospheric Sciences (CFCAS). The authors also thank Rick Ketler for important technical contributions.

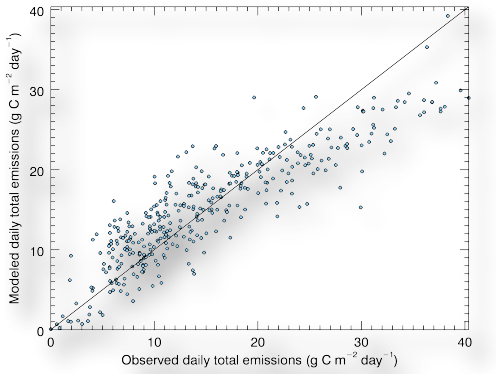

Figure 7. Comparison of observed and modeled daily emission totals for May 2011 - May 2012 (r^2 = 0.78). The 1:1 line is shown in black.

6. References

1. Grimmond C.S.B., Christen A., (2012). Flux measurements in urban ecosystems, Invited article in FluxLetter – Newsetter of Fluxnet, Vol.5 (1), p. 1-7
2. Schmid, H.P. (1994). Source areas for scalars and scalar fluxes. Boundary-Layer Meteorology, 67, 293-318
3. Schmid, H.P., C.R. Lloyd (1999). Spatial representativeness and the location bias of flux footprints over inhomogeneous areas. Agricultural and Forest Meteorology. 93(3), p. 195-209
4. Stewart I.D., T.R. Oke (2012). 'Local Climate Zones' for urban temperature studies. Bulletin of the American Meteorological Society. doi: 10.1175/BAMS-D-11-00019.1
5. Crawford, B., Christen, A., and Ketler, R. (2010). Eddy covariance data processing and quality control procedures, EPiCC Technical Report No.1.
6. Tooke, T., Coops, N., Goodwin, N., and Voogt, J. (2009). Extracting urban vegetation characteristics using spectral mixture analysis and decision tree classifications. Remote Sensing of Environment, 113(2):398–407.
7. Kormann, R. and Meixner, F. (2001). An analytical footprint model for non- neutral stratification. Boundary-Layer Meteorology, 99(2):207–224.
8. Velasco E., M. Roth (2010). Cities as net sources of CO2: Review of atmospheric CO_2 exchange in urban environments measured by eddy covariance technique. Geography Compass, 4(9), 1238-1259
9. Christen, A., N.C. Coops, B.R. Crawford, R. Kellet, K.N. Liss, I. Olchovski, T.R. Tooke, M van der Laan, J.A. Voogt. (2011) Validation of modeled carbon-dioxide emissions from an urban neighborhood with direct eddy-covariance measurements. Atmospheric Environment, 45,33,6057-6069
10. Lloyd J., and Taylor, J.A., (1994): On the temperature dependence of soil respiration. Functional Ecology, 8, 315-323.
11. Liss K., Crawford B., Jassal R., Siemens C., Christen A. (2009): 'Soil respiration in suburban lawns and its response to varying management and irrigation regimes' Proc. of the AMS Eighth Conference on the Urban Environment, Phoenix, AZ, January 11-15, 2009.
12. Ogren E., Evans J. R. (1993) 'Photosynthetic light-response curves, 1. The influence of CO_2 partial pressure and leaf inversion' Planta, 189: 182-190.